Physics Letters A 374 (2010) 2628–2635

Contents lists available at ScienceDirect

Physics Letters A

www.elsevier.com/locate/pla

Periodic window arising in the parameter space of an impact oscillator

E.S. Medeiros [a,*], S.L.T. de Souza [b], R.O. Medrano-T [a], I.L. Caldas [a]

[a] Instituto de Física, Universidade de São Paulo, São Paulo, Brazil
[b] Universidade Federal São João del-Rei, Campus Alto Paraopeba, Minas Gerais, Brazil

ARTICLE INFO

Article history:
Received 28 October 2009
Received in revised form 8 April 2010
Accepted 19 April 2010
Available online 21 April 2010
Communicated by A.R. Bishop

Keywords:
Impact oscillator
Controlling chaos
Parameter space
Nonfeedback method

ABSTRACT

In the bi-dimensional parameter space of an impact-pair system, shrimp-shaped periodic windows are embedded in chaotic regions. We show that a weak periodic forcing generates new periodic windows near the unperturbed one with its shape and periodicity. Thus, the new periodic windows are parameter range extensions for which the controlled periodic oscillations substitute the chaotic oscillations. We identify periodic and chaotic attractors by their largest Lyapunov exponents.

1. Introduction

For experimental [1,2] and theoretical [3–5] classical dynamical systems, parameters with chaotic and periodic attractors are usually represented in bi-dimensional parameter spaces. Generally, in these spaces periodic windows with typical shape [6], called shrimps [7], embedded in chaotic regions have been observed for several systems such as the CO_2 laser model [8], the Colpitts oscillator [9], the associative memory model [10], the Rössler system [11], the mesoscopic electroencephalogram model [12], the inductorless Chua's circuit [13], and the impact-pair system [14]. Each periodic window has a central isoperiodic body with superstable lines where the largest Lyapunov exponent reaches its minimum. In the parameter space, the transitions to chaos can be identified as routes from the shrimp central body to the chaotic region [3].

One desirable property associated with periodical attractors is the facility for the prediction of the future state of the system, in contrast with chaotic attractors. Whenever this inherent difficulty is regarded as undesirable, chaotic attractors are usually avoided in many systems designed for technological applications. It turns out, however, that chaotic behavior, if properly handled, can be of practical interest in real-world applications. To accomplish that, two main methods have been applied to control chaos and avoid undesirable chaotic effects in classical systems [15], i.e., to generate controlled periodical attractors from chaotic attractors. One method is the Ott, Grebogi, and Yorke (OGY) [16], applied to stabilize unstable periodic orbits embedded in a chaotic attractor. Another method is the chaos control by the application of additional small periodic perturbations [17–19]. In these methods, the attention is usually focused on adequate limited ranges of control parameters. However, besides the assessment of the control in large parameter ranges, the onset of periodic windows of controlled orbits, in bi-dimensional parameter spaces, have not been investigated yet.

In this work, we investigate the alterations, in the parameter space, due to a small perturbation in an impact oscillator, known as impact-pair [20]. The impact oscillators appear in a wide range of practical problems in the engineering context [21–25]. In physics, the well-know Fermi–Ulam model [26,27] is the classical example of an impact oscillator. For the impact-pair system, a wide variety of nonlinear phenomena have been identified like diverse kinds of bifurcations, chaotic regimes, crises, coexisting of attractors, basins of attraction with fractal boundaries, basins of attraction with band accumulations, basin hopping, and shrimp-shaped windows in the parameter space [14,28]. In addition, the OGY method was applied to control chaotic regimes [29].

By applying a small perturbation we control orbits for parameters in the chaotic region near an unperturbed shrimp. In the parameter space, a new shrimp-shaped periodic window arises in the region with controlled periodic orbits. This new window has a shape similar to the original one, is localized in its neighborhood and presents the same periodicity and similar superstable lines. Thus, the new controlled periodic windows extend the parameters range for which the system can have periodic oscillations.

This Letter is organized as follows: In Sections 2 and 3 we introduce a dynamical description of the impact-pair model. In Sec-

* Corresponding author. Tel.: +55 11 3091 6914; fax: +55 11 3091 6706.
E-mail address: esm@if.usp.br (E.S. Medeiros).

0375-9601/$ – see front matter
doi:10.1016/j.physleta.2010.04.045

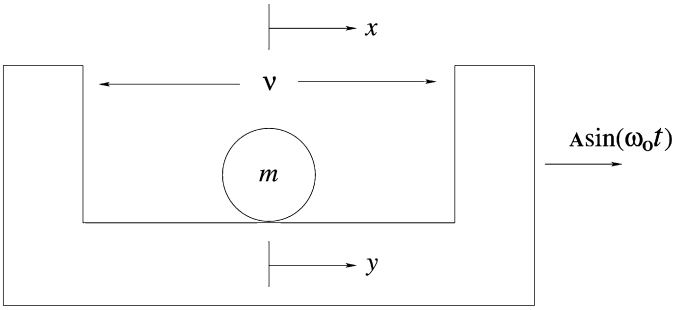

Fig. 1. Schematic of the impact oscillator.

tion 4 we present the changes observed in the parameter space due to the applied small perturbation. In Section 5 we summarize our main conclusions.

2. Impact oscillator

In this section, we describe the theoretical model of the impact-pair system [21]. The system, shown schematically in Fig. 1, is composed of a point mass m and one-dimensional box with a gap of length ν. The mass displacement is denoted by x, in the laboratory coordinates system, and y with reference to the box middle point. The mass m is free to move inside the gap and the motion of the box is described by a periodic function, $e(t) = A\sin(\omega_0 t)$.

An equation of motion and an impact law govern the dynamics of the point mass inside the box.

The equation of motion of the mass m in the laboratory coordinate system is:

$$\ddot{x} = 0. \tag{1}$$

This equation can be solved analytically for the initial conditions $x(t_0) = x_0$ and $\dot{x}(t_0) = \dot{x}_0$:

$$\begin{aligned} x(t) &= x_0 + (t - t_0)\dot{x}_0, \\ \dot{x}(t) &= \dot{x}_0. \end{aligned} \tag{2}$$

To determine the mass position at the impact instant we introduce the coordinate y of a referential in the box:

$$x(t) = y(t) + e(t). \tag{3}$$

Substituting Eq. (3) into Eq. (2):

$$\begin{aligned} y(t) &= y_0 + e(t_0) - e(t) + \big[\dot{y}_0 + \dot{e}(t_0)\big](t - t_0), \\ \dot{y}(t) &= \dot{y}_0 + \dot{e}(t_0) - \dot{e}(t). \end{aligned} \tag{4}$$

This solution is valid between successive impacts, that occurs at $|y| = \nu/2$. We use the Newton's law for impacts to determine the new initial conditions:

$$t_0 = t, \qquad y_0 = y, \qquad \dot{y}_0 = -r\dot{y}. \tag{5}$$

To calculate the Lyapunov exponents for this system, we use the transcendental map [30] obtained by introducing Eq. (5) in Eq. (4):

$$\begin{aligned} y_{n+1} &= y_n + e(t_n) - e(t_{n+1}) + \big[-r\dot{y}_n + \dot{e}(t_n)\big](t_{n+1} - t_n), \\ \dot{y}_{n+1} &= -r\dot{y}_n + \dot{e}(t_n) - \dot{e}(t_{n+1}), \end{aligned} \tag{6}$$

where n indicates the variable values just before the impact instant.

The two-dimensional Lyapunov exponents are obtained with the following expression [30]:

$$\lambda_j = \lim_{N\to\infty} \frac{1}{N} \ln\big|\Delta_j^N\big|, \quad j = 1, 2, \tag{7}$$

where $|\Delta_j^N|$ are the eigenvalues of the matrix M, that is given by:

$$M = \prod_{n=1}^{N} J^n. \tag{8}$$

The J^n is the Jacobian matrix of the time interval between the n-th and $(n+1)$-th impacts of the transcendental map. The product of the Jacobian matrix above can be impracticable due to numerical overflow of its elements. Then we applied a rotation to triangulate it, and the product Eq. (8) is done in the diagonal elements. After that the Lyapunov exponents are computed by:

$$\lambda_j = \lim_{N\to\infty} \frac{1}{N} \sum_{n=1}^{N} \ln\big|a_j^n\big|, \quad j = 1, 2, \tag{9}$$

where $|a_j^N|$ are the eigenvalues of the triangulated Jacobian.

3. Dynamics of the impact oscillator

We obtain the numerical solutions $y(t)$ and the velocity $\dot{y}(t)$ from Eqs. (4) and (5). With these solutions we calculate the largest Lyapunov exponent from Eq. (9). The limit in Eq. (9) is performed until an adequate convergence of the Lyapunov exponents. To guarantee that, we choose in this work a transient scenario where the 60 000 first impacts are neglected. To obtain the results presented in this Letter, we fix the driven frequency $\omega_0 = 1$, the gap length of the box $\nu = 2$, and analyze the dynamic changes varying two control parameters: A, the driven amplitude, and r, the restitution coefficient.

Initially, we present some dynamical aspects of the model without the control. To do that, we obtain bifurcation diagrams and the largest Lyapunov exponents for chosen ranges of parameters A, for which several bifurcations are identified.

To obtain Fig. 2(a), we consider stroboscopic maps ($Time - 2\pi$), from solutions of Eqs. (4) and (5), by varying the parameter A in the interval $1.400 < A < 1.434$ with $r = 0.524072$, neglecting the transient as mentioned before. In this figure we only show the evolution of one attractor. In particular, from $A = 1.416$ to $A = 1.434$, we identify a chaotic attractor with several periodic windows. Fig. 2(b) shows the largest Lyapunov exponent variation obtained by the transcendental map given by Eqs. (6) and (7).

We are interested in controlling chaotic attractors for parameters A and r close periodic windows in the parameter space. For that, we choose the parameters $A = 1.422710$ and $r = 0.524072$ and show, in Fig. 3, for the chaotic attractor to be controlled, the velocity $\dot{y}(t)$ and displacement $y(t)$ at the stroboscopic time.

The periodic windows of the unperturbed system can be better visualized in the parameter space diagram of Fig. 4. To obtain that, we evaluate the Lyapunov exponent for a grid (800×800) of parameters A and r. Parameters with chaotic and periodic behavior are represented, respectively, in yellow (online) and green (online). The periodic windows consist of shrimp-shaped areas. In Fig. 4 blue points (online) indicate parameters with the lowest Lyapunov exponents, inside the windows, corresponding to superstable periodic orbits.

We choose two areas indicated by squares in Fig. 4 to better investigate some orbit properties considered in this Letter. Thus, Fig. 5 shows the magnification of the left square indicated in Fig. 4. The cross in Fig. 5 demarks the parameters corresponding to the chaotic attractor shown in Fig. 3, and the black point corresponds to a periodic attractor ($A = 1.425660$ and $r = 0.526209$) inside the periodic window. These two attractors will

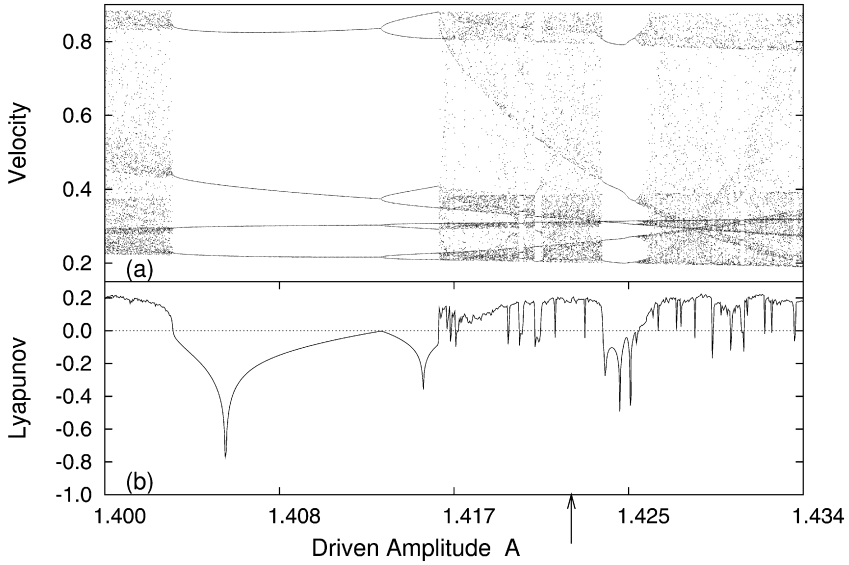

Fig. 2. (a) Bifurcation diagram for the velocity ($Time - 2\pi$) varying the driven amplitude (A), for $r = 0.524072$. (b) Largest Lyapunov exponent calculated for the same parameters of (a). $\omega_0 = 1$, $\nu = 2$. The arrow indicates the parameters ($A = 1.422710$) of the attractors chosen to be controlled.

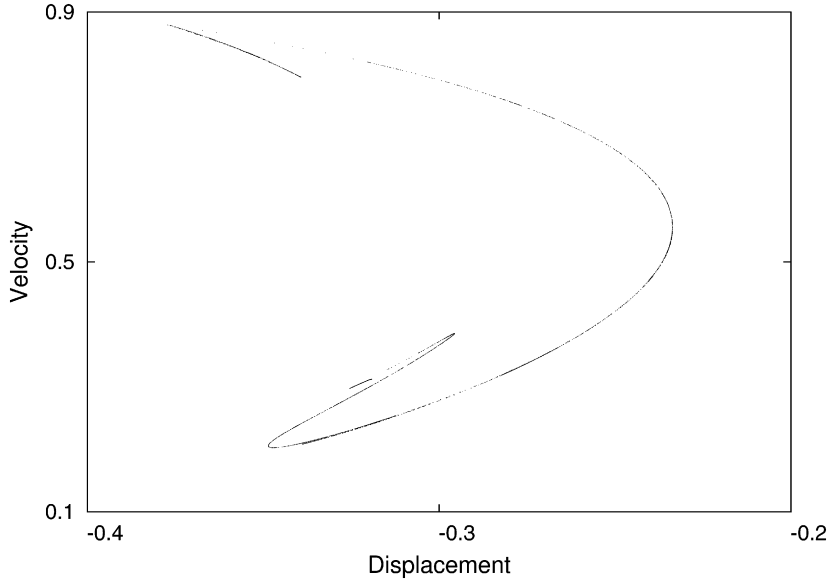

Fig. 3. Stroboscopic map ($Time - 2\pi$) of the chaotic attractor (to be controlled) for $A = 1.422710$ and $r = 0.524072$. $\omega_0 = 1$, $\nu = 2$.

be considered to present the control procedure used in this Letter.

4. Changes in parameter space by a small perturbation

In this section, we investigate the control of chaotic attractors of the impact-pair system by using an external harmonic forcing with small amplitude. This nonfeedback method is applied for chaotic orbits with parameters near a periodic window. Our main interest is to verify the robustness of the controlled orbit in the parameter space, i.e., the observation of a periodic window in the region where the unperturbed chaotic attractor was.

In order to control a chaotic orbit, we modify the original forcing by adding a second term:

$$e(t) = A\sin(\omega_0 t) + B\sin(\omega t), \tag{10}$$

where B is the control amplitude and ω is the control frequency.

To show the applicability of the small amplitude control, we obtain the bifurcation diagram of Fig. 6(a), in terms of the perturbing amplitude, for the fixed chaotic parameter $A = 1.422710$ and $r = 0.524072$ corresponding to the crossed point of Fig. 5. This bifurcation diagram and the corresponding largest Lyapunov exponent in Fig. 6(b) were obtained in a similar way as that of Fig. 2. In Fig. 6 we observe that the parameter B variation technique conducts the system to a 4-period orbit. However, larger values of the parameter B (not shown in Fig. 6) can lead the system to low periodic orbits.

Other values of ω could be used to control the chaotic attractor driven by the original forcing with the frequency $\omega_0 = 1$. To show that we present in Fig. 7 a parameter space $\omega_0 \times \omega$ obtained by calculating the Lyapunov exponent of the perturbed attractor. In this figure, points in the green line represent parameters with negative Lyapunov exponent while points in the yellow area represent parameters for which the perturbed attractors remain chaotic.

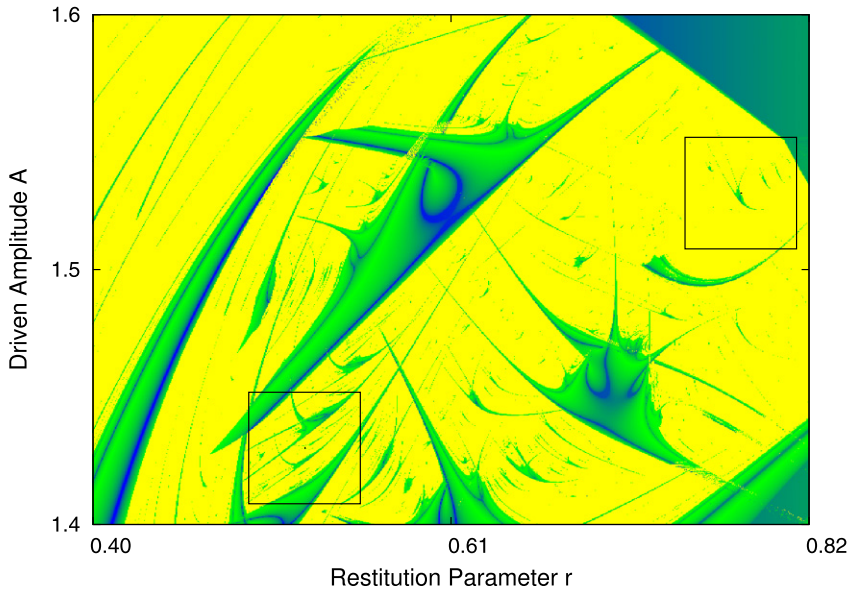

Fig. 4. (Color online.) Bi-dimensional parameter space diagram of the unperturbed system for a grid of parameters A and r. $\omega_0 = 1$, $\nu = 2$. Periodic (chaotic) attractors are in green (yellow). The squares indicate the area amplified in Fig. 5 and in Fig. 9.

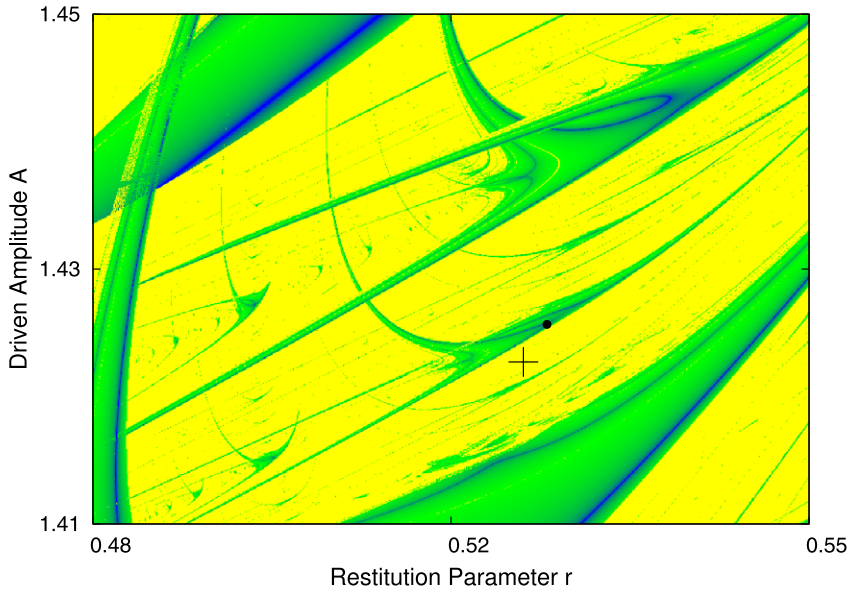

Fig. 5. (Color online.) Magnification of the left square indicated in Fig. 4. The cross indicates the parameter values of the chaotic attractor to be controlled and the black point indicates a periodic attractor inside a shrimp.

Next, we present in Fig. 8, the perturbed parameter space diagram, in terms of A and r, where the color representations are the same of Fig. 4. The cross mark indicates the A and r parameter values of Fig. 3 chaotic attractor chosen to be controlled.

Fig. 8 shows parameter spaces for two different values of forcing amplitude control B. In the first case (a) the parameter space is obtained for $B = 0.0025$. We observe that the chosen chaotic attractor is not yet controlled, but even so a new shrimp-shaped periodic window arises in the neighborhood of the point correspondent to the analyzed orbit chosen to be controlled. In other words, the chosen parameters still remains outside the generated shrimp formed by controlled orbits. We observed that, increasing B, the new shrimp approaches the chosen point and the control is achieved. This result can be seen in the second case (b), for $B = 0.0045$, for which the chosen parameters are in the superstable orbit region of the new shrimp and, consequently, the controlled orbit has the same period of the superstable orbit of the generated shrimp. We note that the old periodic window is displaced as B is varied, and points representing a periodic attractor change their color to represent chaotic attractors, as the black point marked in Fig. 8(a) and in Fig. 8(b).

A magnification of the right square of Fig. 4 is shown in Fig. 9(a). This parameter space amplified area contains periodic and chaotic attractors. The attractor alterations resulting from application of a weak periodic forcing (with $B = 0.0007$ and $\omega = 2$) are shown in Fig. 9(b). In this last figure we observe another example of a new periodic window arising. Namely, the main shrimp in Fig. 9(a) appears duplicated in Fig. 9(b) around its unperturbed place. In Fig. 9, the cross indicates the parameters of the chaotic attractor to be controlled ($A = 1.523030$ and $r = 0.782943$) and the parameters of a periodic attractor ($A = 1.527820$ and $r =$

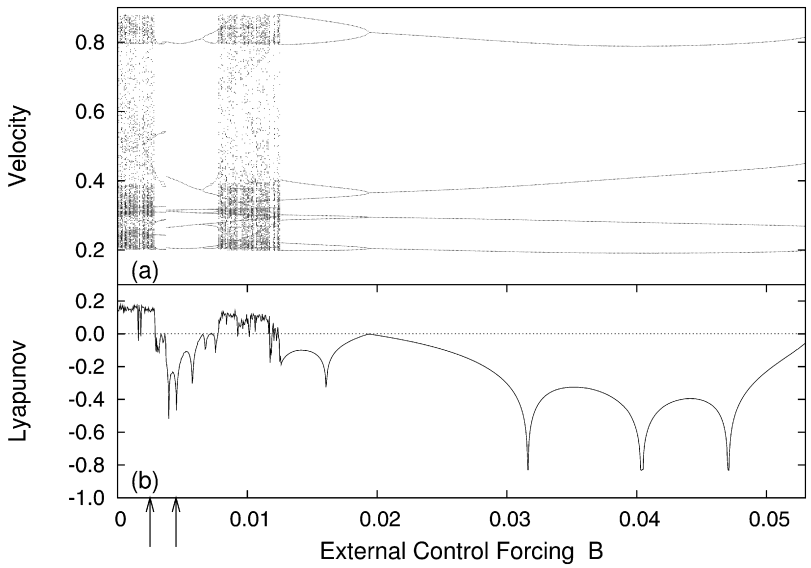

Fig. 6. (a) Bifurcation diagram for the velocity ($Time - 2\pi$) varying the external control forcing (B), for $A = 1.422710$ and $r = 0.524072$. (b) Largest Lyapunov exponent calculated for the same parameters of (a). $\omega_0 = 1$, $\omega = 0.5$ and $\nu = 2$. The arrows indicate the control parameters values ($B = 0.0025$ and $B = 0.0045$) used in Fig. 8.

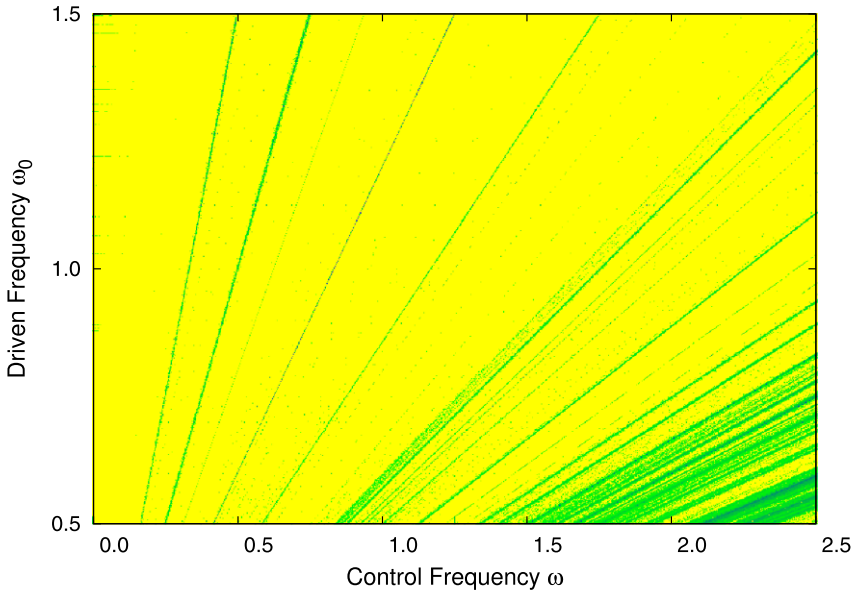

Fig. 7. (Color online.) Parameter space $\omega_0 \times \omega$ of the natural and driven frequencies. Controlled periodic (chaotic) attractors are in green (yellow). $A = 1.422710$, $r = 0.524072$ and $B = 0.0045$.

0.779605) inside the unperturbed shrimp are indicated in Fig. 9(a) by a black point.

In general, application of feedback control methods stabilizes unstable periodic orbits embedded in the original chaotic attractors and, therefore, do not change the attractors of the controlled systems [15]. In our case, we apply a nonfeedback method that slightly modifies the chaotic attractor to a periodic one, which is located (in the parameter space) in the neighborhood of the initial attractor. This kind of attractor alteration is typical of nonfeedback methods [15].

To be more specific, we show in the stroboscopic map ($Time - 2\pi$) of Fig. 10 that the controlled attractor assumes the periodicity (6-period) of a pre-existing periodic attractor (black point of Fig. 5) in the shrimp located in the neighborhood of the chosen chaotic orbit parameters. In fact, as shown in Fig. 10, the same velocity and displacement are obtained for the controlled orbit, for given parameters inside the new generated shrimp, and the periodic orbit for parameters located in the original shrimp. These values, shown in Fig. 10, obtained for the superstable orbits of the mentioned shrimps, are indistinguishable. The observed correspondence is due to the shrimps resemblance observed in Fig. 8.

Next, in Fig. 11(a) we present in phase space a piece of the unperturbed chaotic attractor (observed for parameters indicated by the cross of Fig. 5), in black, superposed to the unperturbed periodic attractor in red (for parameters indicated by the black point of Fig. 5). Complementary, we show in Fig. 11(b) how these two attractors are modified by the applied small perturbation. Thus, we can recognize that both periodic orbits of Fig. 11 are embedded in chaotic attractors.

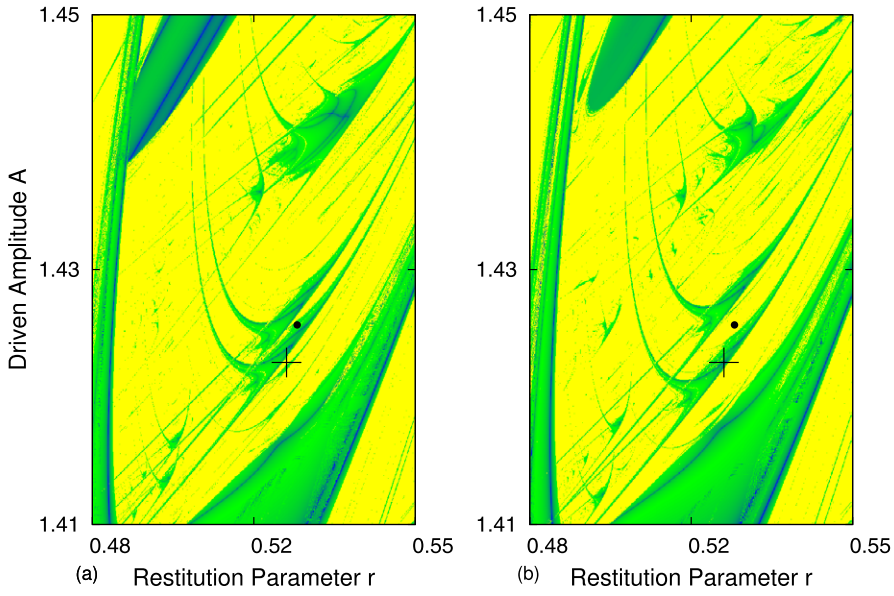

Fig. 8. (Color online.) Perturbed parameter space for the area indicated by the left square of Fig. 4. The parameters of the chaotic orbit to be controlled are indicated by a cross mark (also shown in Fig. 3). (a) For external control forcing $B = 0.0025$ a new periodic window arises. (b) For $B = 0.0045$, the central new shrimp body reaches the cross mark. $\omega_0 = 1$, $\omega = 0.5$ and $\nu = 2$.

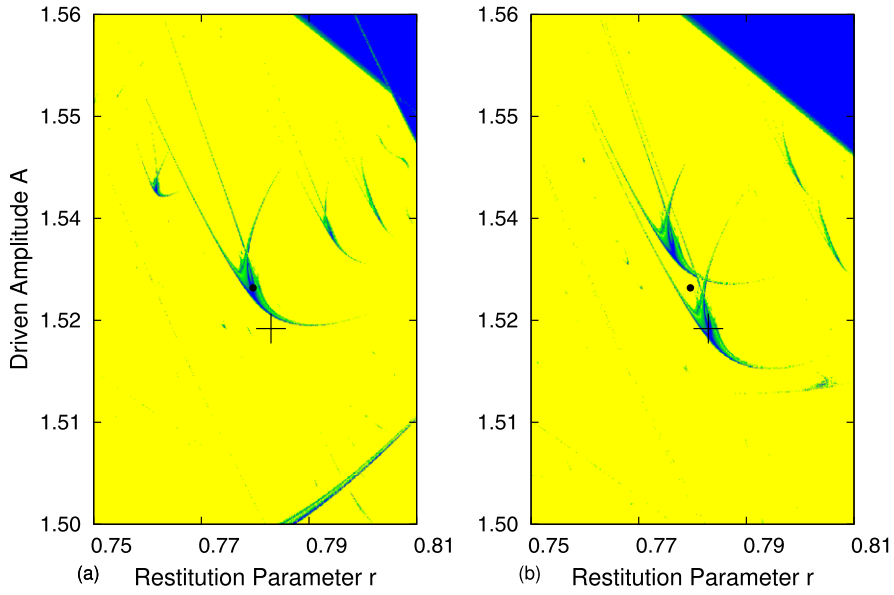

Fig. 9. (Color online.) (a) Parameter space magnification of the area indicated by the right square of Fig. 4. The parameters of the chaotic orbit to be controlled are indicated by a cross mark. (b) Perturbed parameter space of the same area of (a), for external control forcing $B = 0.0007$, where a new periodic window arises. $\omega_0 = 1$, $\omega = 2.0$ and $\nu = 2$.

5. Conclusions

We investigate the control of chaos for impact-pair system driven by a small harmonic forcing. To identify periodic and chaotic regions in the parameter space diagram, we compute the largest Lyapunov exponents for the attractors in the considered parameter ranges. We identify shrimp-shaped periodic windows immersed into a chaotic region.

The parameter space is much modified whenever the small amplitude forcing is applied. New similar periodic windows arise in the neighborhood of the original windows. We verify that periodic orbits are similar (and with the same periodicity) for parameters inside the original and the new periodic windows.

Moreover, we show how the chaotic attractors change with the increasing amplitude forcing until they become controlled and reach periodic orbits existing for parameters in the unperturbed window. This evolution corresponds to a displacement of the new window until it reaches the parameters of the chosen chaotic orbit to be controlled.

One relevant aspect we did not analyze is how the shrimp-shaped windows form and evolve; in particular it would be worthwhile to investigate the possible stabilization, by the parametric driven, of the unstable periodic orbits embedded in the chaotic attractors.

As far we have found in the literature, shrimps are very common in dissipative systems with periodic and chaotic attractors. We believe that our results concerning the periodic window aris-

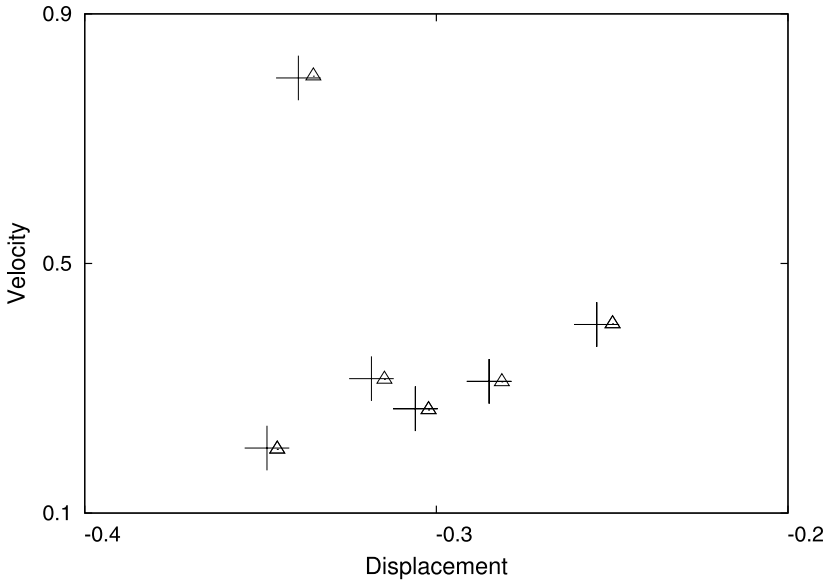

Fig. 10. Superposition of velocity and displacement at the stroboscopic time for the controlled periodic attractor (triangle symbol) for $B = 0.0045$ and another pre-existing periodic attractor (plus symbol) with parameters close to those of the controlled attractor. $\omega_0 = 1$, $\omega = 0.5$, $\nu = 2$.

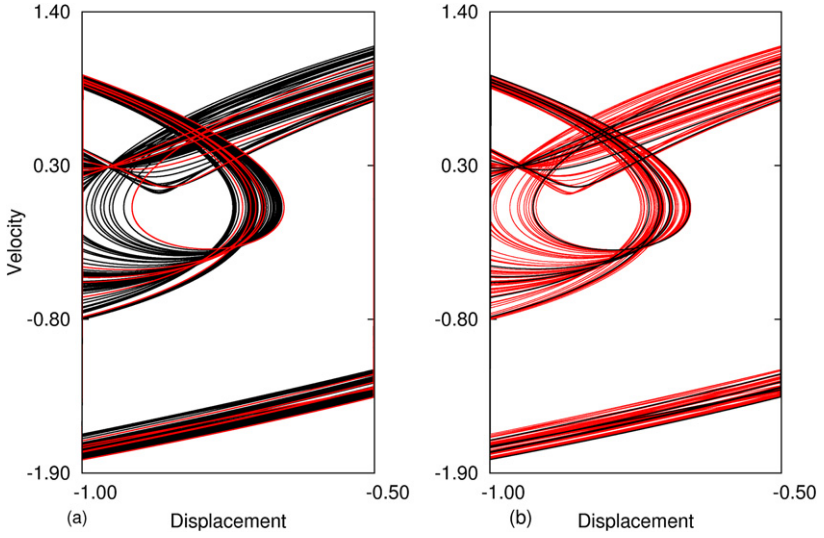

Fig. 11. (Color online.) (a) Superposition of the chaotic attractor (black) to be controlled ($A = 1.422710$ and $r = 0.524072$) and an unperturbed periodic attractor (red) ($A = 1.425660$ and $r = 0.526209$). (b) Superposition of these attractors modified by the perturbation (the modified attractors are indicated by the same colors they have in (a)). $\omega_0 = 1$, $\omega = 0.5$ and $\nu = 2$.

ing will be verified even in more sophisticated controlled models as those assuming a friction law between the mass and the box surface or considering an accurate impact law such as the Poisson law or energetic laws.

Acknowledgements

This work was made possible by partial financial support from the following Brazilian government agencies: FAPESP, CNPq, and Capes.

References

[1] J.C.D. Cardoso, H.A. Albuquerque, R.M. Rubinger, Phys. Lett. A 373 (2009) 2050.
[2] D.M. Maranhão, M.S. Baptista, J.C. Sartorelli, I.L. Caldas, Phys. Rev. E 77 (2008) 037202.
[3] J.A.C. Gallas, Phys. Rev. Lett. 70 (1993) 2714.
[4] K. Ullmann, I.L. Caldas, Chaos Solitons Fractals 7 (1996) 1913.
[5] M.S. Baptista, I.L. Caldas, Chaos Solitons Fractals 7 (1996) 325.
[6] E.N. Lorenz, Phys. D 237 (2008) 1689.
[7] J.A.C. Gallas, Phys. A 202 (1994) 196.
[8] C. Bonatto, J.C. Garreau, J.A.C. Gallas, Phys. Rev. Lett. 95 (2005) 143905.
[9] O. De Feo, G.M. Maggio, Int. J. Bifur. Chaos 13 (2003) 2917.
[10] M. Kawamura, R. Tokunaga, M. Okada, Phys. Rev. E 70 (2004) 046210.
[11] V. Castro, M. Monti, W.B. Pardo, J.A. Walkenstein, E. Rosa Jr., Int. J. Bifur. Chaos 17 (2007) 965.
[12] L. van Veen, D.T.J. Liley, Phys. Rev. Lett. 97 (2006) 208101.
[13] H.A. Albuquerque, R.M. Rubinger, P.C. Rech, Phys. Lett. A 372 (2008) 4793.
[14] S.L.T. de Souza, I.L. Caldas, R.L. Viana, Math. Probl. Eng. 2009 (2009) 290356.
[15] T. Kapitaniak, J. Brindley, K. Czolczynski, in: G. Chen (Ed.), Controlling Chaos and Bifurcations in Engineering Systems, CRC Press LLC, Boca Raton, 1999, pp. 71–86.
[16] O. Edward, C. Grebogi, J.A. Yorke, Phys. Rev. Lett. 64 (1990) 1196.
[17] R. Lima, M. Pettini, Phys. Rev. A 41 (1990) 726.
[18] Y. Braiman, I. Goldhirsch, Phys. Rev. Lett. 66 (1991) 2545.
[19] T. Kapitaniak, Chaos Solitons Fractals 2 (1992) 519.

[20] R.P.S. Han, A.C.J. Luo, W. Deng, J. Sound Vibration 181 (1995) 231.
[21] K. Karagiannis, F. Pfeiffer, Nonlinear Dynam. 2 (1991) 367.
[22] J. Ing, E. Pavlovskaia, M. Wiercigroch, Nonlinear Dynam. 46 (2006) 225.
[23] M. Wiercigroch, A.M. Krivtsov, J. Wojewoda, J. Theoret. Appl. Mech. 46 (2008) 715.
[24] S.L.T. de Souza, I.L. Caldas, R.L. Viana, J.M. Balthazar, J. Theoret. Appl. Mech. 46 (2008) 641.
[25] S.L.T. de Souza, I.L. Caldas, R.L. Viana, Chaos Solitons Fractals 32 (2007) 745.
[26] M.A. Lieberman, A.J. Lichtenberg, Phys. Rev. A 5 (1972) 1852.
[27] E.D. Leonel, P.V.E. McClintock, J.K.L. Silva, Phys. Rev. Lett. 93 (2004) 14101.
[28] S.L.T. de Souza, A.M. Batista, I.L. Caldas, R.L. Viana, T. Kapitaniak, Chaos Solitons Fractals 32 (2007) 758.
[29] S.L.T. de Souza, I.L. Caldas, Chaos Solitons Fractals 19 (2004) 171.
[30] S.L.T. de Souza, I.L. Caldas, Chaos Solitons Fractals 19 (2004) 569.